IEEE Access
Multidisciplinary ⋮ Rapid Review ⋮ Open Access Journal

Received October 10, 2020, accepted October 25, 2020, date of publication October 30, 2020, date of current version November 11, 2020.

Digital Object Identifier 10.1109/ACCESS.2020.3035046

Computation of Maximum Voltage Droop in Power Delivery Networks

SEUNGHYUP HAN, OSAMA WAQAR BHATTI, AND MADHAVAN SWAMINATHAN, (Fellow, IEEE)

3D Systems Packaging Research Center (PRC), School of Electrical and Computer Engineering, Georgia Institute of Technology, Atlanta, GA 30332, USA

Corresponding author: Seunghyup Han (seunghyup@gatech.edu)

ABSTRACT Computation of maximum voltage droop in power delivery networks is important for performance estimation. This article proposes a methodology to predict the maximum voltage droop caused by current sources in ICs. We derive the analytical relations and analyze the error in the predicted voltage droop values. Furthermore, we consider the effect of current step rise time on the voltage droop along with error analysis. Results capture the error bounds for the analytical equations derived.

INDEX TERMS Integrated circuit (IC), maximum voltage droop, power delivery network (PDN).

I. INTRODUCTION

Due to the increase in clock frequency and density of transistors in integrated circuits (IC), designing robust power delivery networks (PDN) presents a challenge for today's high-performance systems. The primary purpose of PDN design is to ensure delivery of stable power to ICs. However, loads consuming fast, transient and high current cause large power supply noise and voltage droop resulting in IC malfunction and other issues related to signal integrity and electromagnetic interference (EMI) to other parts of the system. This presents a challenge for managing power supply noise and keeping it below a threshold level.

Consider a typical PDN for a generic high-performance computing system as shown in Fig. 1, consisting of the printed circuit board (PCB), package, and ICs. Several routing paths and interconnections exist that are used to supply the desired power from the voltage regulator module (VRM) to the ICs. For stable power delivery to the load, decoupling capacitors are added near each component thereby reducing the PDN impedance over the frequency range of interest. For any PDN with these configured components and design, the voltage response at the load in PDN depends on the current sources. Therefore, to ensure a stable power supply, it is necessary to predict the voltage response in time domain and the maximum voltage droop depending on the current sources in design stages.

Several studies have focused on the voltage responses depending on PDNs and IC loads, and the results of voltage response form particular current sources are provided using commercial tools [1]–[5]. However, a more intuitive method

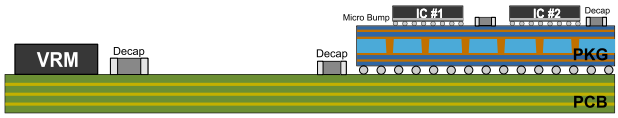

FIGURE 1. Typical PDN model of the high-performance computing system consisting of PCB, package, and ICs.

is required for the prediction of voltage response rather than using simulation tools in the early PDN design stage. In [6]–[8], the expressions for the voltage responses in time domain are derived analytically based on the modeled PDN, thereby providing the intuitive relationship between power supply noise and PDN parameters. However, since only typical pulses are used as current sources, the voltage responses from various types of load current which are representatives of IC operations are not covered. The prediction of maximum voltage droop by analytical calculation has been proposed in [9]. In this approach, three basic types of current sources are proposed, and the maximum voltage droop caused by these at the load are calculated by using simplified equations with PDN parameters. The rationale for using the three forms of current sources in [9] is that these excitations form a current basis where any current excitation can be represented using a combination of impulse, step and periodic excitations. In addition, for PDN characterization, the voltage response and droop from these load currents are the figures of merit since these excitations are based on the typical IC operations [9]. An example of both the current sources and their voltage responses from the load are plotted in Fig. 2. This provides a quick method for estimating voltage droops, and also provide insight into the parameters that need to be optimized in real designs. However, the equations provided in [9] can lead to large errors depending on the component values used since they do not provide any information on the error bounds.

The associate editor coordinating the review of this manuscript and approving it for publication was Bo Pu.

This work is licensed under a Creative Commons Attribution 4.0 License. For more information, see https://creativecommons.org/licenses/by/4.0/

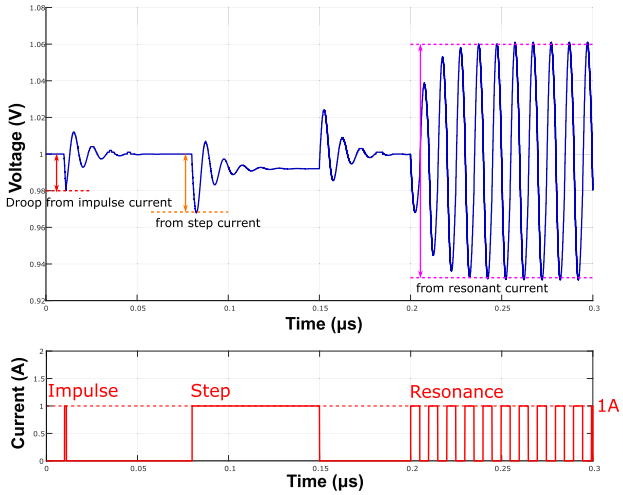

FIGURE 2. Voltage responses caused by step, impulse, and resonant current at the load.

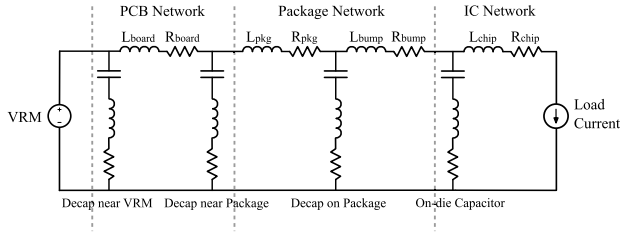

FIGURE 3. Simple equivalent circuit model of the PDN.

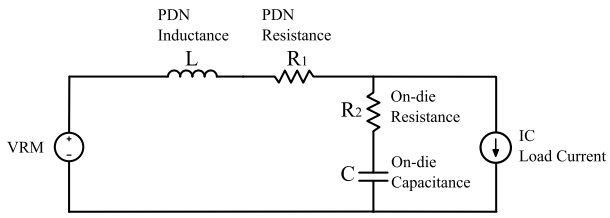

FIGURE 4. Further simplified circuit model of the PDN.

TABLE 1. Parameter values of the simple equivalent PDN circuit.

Parameters		Value
L	PDN inductance	50pH
R_1	PDN resistance	8mΩ
C	On-die capacitance	50nF
R_2	On-die resistance	2mΩ

In this article, we propose a method to compute maximum voltage droops using the three fundamental current sources from ICs, but we re-derive the equations in [9] and validate the associated errors based on simulations. We then modify these equations to minimize errors along with the allowable usable range for the component parameters. For verification, the proposed method is applied to the prediction of voltage droop from an arbitrary current source from ICs. In addition, we quantify the error bounds of the simplified equations, and include current rise time as a variable parameter, which can have a significant effect on the level of voltage droop.

This article is organized as follows. In Section II, we identify the boundary conditions for the equations and validate the associated error. The equations are then re-derived in Section III and then modified to reduce error. Section IV analyzes the error bounds for each equation followed by Section V, where the effect of current rise time is discussed. Finally, the conclusion is presented in Section VI.

II. PROBLEM FORMULATION

To analyze the PDN, the general approach is to use an equivalent circuit model to represent the actual network, as shown in Fig. 3 [10]. From the perspective of an IC and system designer, Fig. 3 can be further simplified into Fig. 4 to capture the impedance peak, which is dominant to voltage droops in ICs and is created by the parallel resonance between the on-die capacitance C and PDN inductance L. Fig. 4 closely represents a system which assumes that all other impedance peaks have been suppressed below the target impedance using appropriate strategies such as placement of package and board level decoupling capacitors [9], [11]. In this article, we use Fig. 4 as the starting point for our analyses similar to [9].

As indicated earlier, Fig. 2 shows the voltage droops at the load caused by three different 1A current sources. We obtain them by simulating the PDN circuit in Fig. 4. A typical set of circuit parameter values used in PDNs are provided in Table 1. Each dotted line in Fig. 2 represents the estimated maximum voltage droop by using the equations described in [9]:

$$V_{impulse} = \frac{1}{C} \cdot \frac{I_{avg.}}{f_{clk}} \tag{1}$$

$$V_{step} = Z_0 \cdot I_{step} \tag{2}$$

$$V_{resonance} = Z_{peak} \cdot \frac{4}{\pi} \cdot I_{resonance} \tag{3}$$

where I_{avg}, f_{clk}, I_{step}, and $I_{resonance}$ are the average of impulse current, clock frequency, magnitude of step and resonant current, respectively. The impulse, step and resonant current sources from the load cause the voltage droops V_{impuse}, V_{step}, and $V_{resonance}$, respectively. In the above equations, other parameters are defined as follows:

$$f_0 = \frac{1}{2\pi\sqrt{LC}} \tag{4}$$

$$Z_0 = \sqrt{\frac{L}{C}} \tag{5}$$

$$Q = \frac{Z_0}{R_{total}} \tag{6}$$

$$Z_{peak} = Z_0 \cdot Q \tag{7}$$

where f_0, Z_0, Q, Z_{peak}, and R_{total} are the resonant frequency, characteristic impedance, quality factor, peak impedance and the sum of R_1 and R_2 [9], [11].

Table 2 compares the simulated and calculated maximum voltage droop values. Here, the agreement is close meaning that the equations are valid based on the component values used. The small deviations in Table 2 are caused by the PDN and on-die resistance in the PDN circuit, which are ignored in (1)-(3), meaning that as these resistance values

TABLE 2. Comparison of the maximum voltage droops from equations and simulations.

Current source	Simulated value	Calculated value	Error
Impulse current	19.99mV	20.00mV	0.05%
Step current	32.05mV	31.62mV	1.34%
Resonant current	129.39mV	127.32mV	1.60%

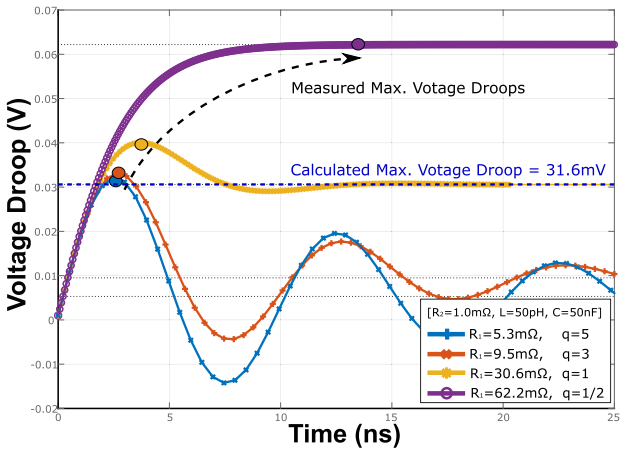

(a)

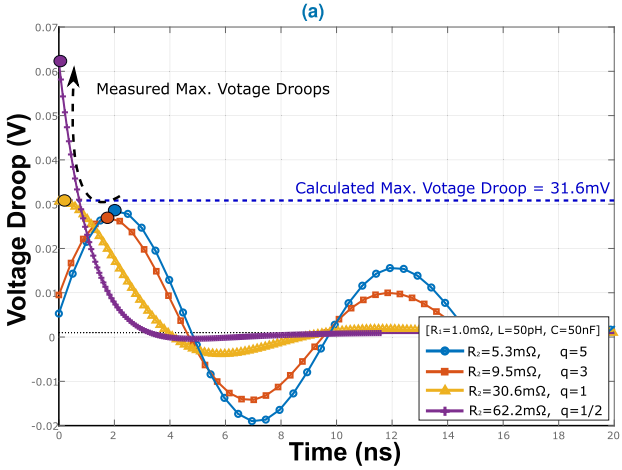

(b)

FIGURE 5. Change of the voltage droop from a step current, (a) R_1 increasing, and (b) R_2 increasing.

reduce, the error converges towards zero. However, as these resistance values increase, (1)-(3) become invalid. This effect is illustrated in Fig. 5, 6, and 7. The solid lines represent the voltage droop under different PDN or on-die resistances and the dotted lines indicate the calculated maximum voltage droop level using the equations, which is constant with resistance change. When both PDN and on-die resistance are less than 10mΩ, the maximum voltage droop is close to the computed values. However, as one of the resistance increases above 10mΩ (which is possible in a PDN), the deviation between calculated and simulated values become significant. Hence, modifications to these equations are required, which are discussed in the next section.

III. RIGOROUS SOLUTION

In this section, we first derive the equations with the resistance in the PDN circuit assumed to be zero. Secondly,

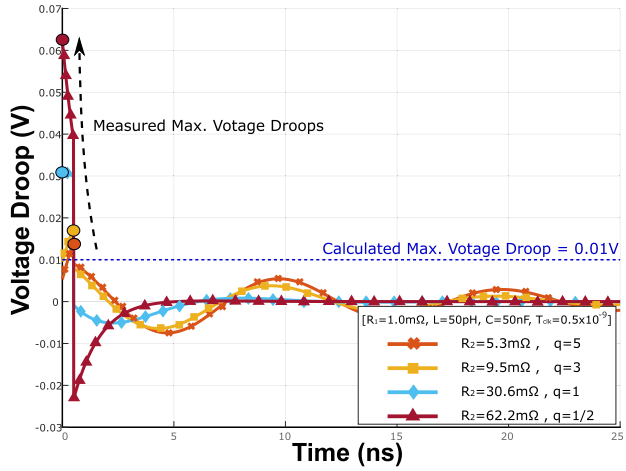

FIGURE 6. Change of the voltage droop from an impulse current with an increase of R_2.

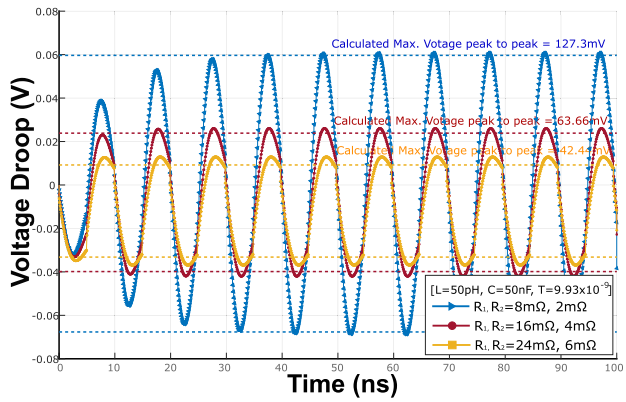

FIGURE 7. Change of the voltage droop from a resonant current with an increase of R_1 and R_2.

we take into account the resistance and provide modified equations for a more rigorous solution. We then introduce factors that need additional consideration compared to the parameters used earlier. We also propose an additional parameter (current pulse time duration) in addition to the component parameters for using the voltage droop equations to compute maximum voltage droop.

A. STEP CURRENT

Assuming negligible resistance, the impedance transfer function $H(s)$ of the equivalent PDN circuit in Fig. 4 can be written as:

$$H(s) = \frac{V(s)}{I(s)} = \frac{\frac{1}{C}s}{s^2 + \frac{1}{LC}} \tag{8}$$

Using the step current source, the voltage response can be derived to be:

$$\begin{aligned} v^*(t)_{step} &= \sqrt{\frac{L}{C}} \cdot sin\left(\frac{1}{\sqrt{LC}}t\right) \cdot I_{step} \\ &= Z_0 \cdot I_{step} \cdot sin(2\pi f_0 \cdot t) \end{aligned} \tag{9}$$

Here, the voltage response is sinusoidal with resonant frequency f_0 and amplitude $Z_0 * I_{step}$. From (9), the maximum voltage droop is as given in (2).

When the resistances are included, the transfer function of the PDN circuit becomes:

$$H(s) = \frac{V(s)}{I(s)} = \frac{R_2 \cdot s^2 + \frac{L+R_1R_2C}{LC} \cdot s + \frac{R_1}{LC}}{s^2 + \frac{R_1+R_2}{L} \cdot s + \frac{1}{LC}} \tag{10}$$

Using the unit step function for the current, the voltage response in time domain can be derived as:

$$\begin{aligned} v(t)_{step} &= R_1 + (R_2 - R_1) \cdot e^{-\left(\frac{R_1+R_2}{2L}\right)\cdot t} \\ &\cdot \left\{ cos\left(\sqrt{\frac{1}{LC} - \frac{(R_1+R_2)^2}{4L^2}} \cdot t\right) - \frac{\frac{R_1+R_2}{2L} - \frac{L-CR_1^2}{LC(R_2-R_1)}}{\sqrt{\frac{1}{LC} - \frac{(R_1+R_2)^2}{4L^2}}} \right. \\ &\left. \cdot sin\left(\sqrt{\frac{1}{LC} - \frac{(R_1+R_2)^2}{4L^2}} \cdot t\right) \right\} \end{aligned} \tag{11}$$

Since Fig. 4 is a second-order circuit model and the voltage response is sinusoidal when (2) is valid, we consider the under-damped case. This requires that:

$$\frac{1}{LC} - \frac{(R_1+R_2)^2}{4L^2} > 0 \tag{12}$$

Substituting (5) and (6) into (12):

$$Q > \frac{1}{2} \tag{13}$$

where the parameter Q is as defined in (6). Using (12), (11) can be further modified and written as:

$$\begin{aligned} v(t)_{step} &= R_1 + (R_2 - R_1) \cdot e^{-(\frac{R_1+R_2}{2L})\cdot t} \\ &\cdot A \cdot \{cos(\sqrt{\frac{1}{LC} - \frac{(R_1+R_2)^2}{4L^2}} \cdot t - \phi) \end{aligned} \tag{14}$$

where

$$A = \sqrt{1 + (-\frac{\frac{R_1+R_2}{2L} - \frac{L-CR_1^2}{LC(R_2-R_1)}}{\sqrt{\frac{1}{LC} - \frac{(R_1+R_2)^2}{4L^2}}})^2} \tag{15}$$

$$\phi = tan^{-1}\left(- \frac{\frac{R_1+R_2}{2L} - \frac{L-CR_1^2}{LC(R_2-R_1)}}{\sqrt{\frac{1}{LC} - \frac{(R_1+R_2)^2}{4L^2}}} \right) \tag{16}$$

Substituting (5), (6) into (14), leads to:

$$\begin{aligned} v(t)_{step} &= R_1 + Z_0 \cdot e^{-\left(\frac{2\pi f_0}{2Q}\right)\cdot t} \cdot \frac{(R_2 - R_1)}{\sqrt{((R_2-R_1)^2}} \\ &\cdot \sqrt{\frac{(1 - \frac{1}{Q^2}\frac{R_1R_2}{(R_1+R_2)^2})^2}{(1 - \frac{1}{4Q^2})}} \\ &\cdot cos\left(2\pi f_0 \cdot \sqrt{1 - \frac{1}{4Q^2}} \cdot t - \phi\right) \end{aligned} \tag{17}$$

Based on (17), the voltage response from a step current source is an exponentially decaying sinusoid with DC droop depending on the resistance R_1. As the resistance decreases, the square root term approaches unity because of the high Q. In this case, the maximum voltage droop is only proportional to the characteristic impedance, Z_0 as in (2). However, as Q decreases, the square root term becomes less than 1, and this equality no longer holds. Therefore, the maximum voltage droop is determined by not just Z_0 but also R_1, R_2, and Q. Due to these additional parameters which may be important in an actual design, the maximum droop calculated can deviate significantly from the result in (2).

B. IMPULSE CURRENT

With the resistance assumed zero, the voltage response to impulse current is:

$$\begin{aligned} v^*(t)_{impulse} &= \frac{1}{C} \cdot cos(\sqrt{\frac{1}{LC}} \cdot t) \\ &= \frac{1}{C} \cdot cos(2\pi f_0 \cdot t) \end{aligned} \tag{18}$$

However, if we consider a practical current pulse, the impulse function needs to be replaced by a single pulse current with a short time duration. Then, the voltage response from the current pulse excitation becomes:

$$V(s)_{impulse} = H(s) \cdot I_{avg} \cdot \left(\frac{1}{s} - \frac{e^{-as}}{s}\right) \tag{19}$$

which in time domain results in:

$$v(t)_{impulse} = \begin{cases} \sqrt{\frac{L}{C}} \cdot sin\left(\frac{1}{\sqrt{LC}}t\right) \cdot I_{avg}, & 0 < t \le a \\ \sqrt{\frac{L}{C}} \left\{ (sin(\frac{1}{\sqrt{LC}}t) \right. \\ \quad \left. - sin(\frac{1}{\sqrt{LC}}(t-a)) \right\} \cdot I_{avg}, & t > a \end{cases} \tag{20}$$

where I_{avg} and a are the average current and time duration of the current pulse, respectively.

For $0 < t \le a$, if the pulse time duration a is small enough, based on the linear approximation, the voltage droop at $t = a$ can be written as:

$$v(0+a) \approx v(0) + v'(a) \cdot a \tag{21}$$

where, $v'(a)$ is

$$v'(a) = \frac{1}{C} \cdot cos\left(\frac{a}{\sqrt{LC}}\right) \cdot I_{avg} \tag{22}$$

Then, the maximum voltage droop when $t = a$ is obtained as:

$$v(a) = \frac{1}{C} \cdot I_{avg} \cdot a \cdot cos\left(\frac{a}{\sqrt{LC}}\right) \tag{23}$$

Since a equals $1/f_{clk}$ and the cosine term approaches unity with small a, the maximum voltage droop is as given in (1).

Similarly, for $t > a$, the voltage response $v(t)$ becomes:

$$\begin{aligned} v(t)_{impulse} &= \sqrt{\frac{L}{C}} \cdot \left\{ \sqrt{(1 - cos\frac{1}{\sqrt{LC}}a)^2 + (sin\frac{1}{\sqrt{LC}}a)^2} \right. \\ &\left. \cdot cos(\frac{1}{\sqrt{LC}}t - \phi) \right\} \cdot I_{avg} \\ &= \sqrt{\frac{L}{C}} \cdot \sqrt{\left(sin\frac{1}{\sqrt{LC}}a\right)^2} \cdot cos(\frac{1}{\sqrt{LC}}t - \phi) \cdot I_{avg} \\ &\approx \frac{1}{C} \cdot I_{avg} \cdot a \cdot cos(\frac{1}{\sqrt{LC}}t - \phi) \end{aligned} \tag{24}$$

where small a is assumed and linear approximation is used. Here, the voltage response is sinusoidal with amplitude $1/C \cdot I_{avg}/f_{clk}$ meaning that the maximum voltage droop is the same as (1).

However, with the resistance included, the voltage response for impulse current excitation becomes:

$$v(t)_{impulse} = R_2 \cdot \delta(t) + \frac{L - R_2^2 C}{LC} \cdot e^{-(\frac{R_1+R_2}{2L})\cdot t} \cdot \left\{ cos\left(\sqrt{\frac{1}{LC} - \frac{(R_1+R_2)^2}{4L^2}} \cdot t\right) - \frac{\frac{R_1+R_2}{2L} - \frac{R_1-R_2}{L-R_2^2 C}}{\sqrt{\frac{1}{LC} - \frac{(R_1+R_2)^2}{4L^2}}} \cdot sin\left(\sqrt{\frac{1}{LC} - \frac{(R_1+R_2)^2}{4L^2}} \cdot t\right) \right\} \tag{25}$$

As mentioned earlier, since the under-damped case is considered, Q is greater than 1/2. Then, (25) can be rewritten as:

$$v(t)_{impulse} = R_2 \cdot \delta(t) + \frac{L - R_2^2 C}{LC} \cdot e^{-(\frac{R_1+R_2}{2L})\cdot t} \cdot A \cdot \left\{ cos\left(\sqrt{\frac{1}{LC} - \frac{(R_1+R_2)^2}{4L^2}} \cdot t - \phi\right) \right\} \tag{26}$$

where the amplitude A and phase ϕ are given by:

$$A = \sqrt{1 + \left(- \frac{\frac{R_1+R_2}{2L} - \frac{R_1-R_2}{L-R_2^2 C}}{\sqrt{\frac{1}{LC} - \frac{(R_1+R_2)^2}{4L^2}}} \right)^2} \tag{27}$$

$$\phi = tan^{-1}\left(- \frac{\frac{R_1+R_2}{2L} - \frac{R_1-R_2}{L-R_2^2 C}}{\sqrt{\frac{1}{LC} - \frac{(R_1+R_2)^2}{4L^2}}} \right) \tag{28}$$

Substituting (4), (5), and (6) into (26), the voltage response can be further expressed as:

$$v(t)_{impulse} = R_2 \cdot \delta(t) + \frac{1}{C} \cdot e^{-\left(\frac{2\pi f_0}{2Q}\right)\cdot t} \cdot \sqrt{\frac{(1 - \frac{1}{Q^2}\frac{R_1 R_2}{(R_1+R_2)^2})^2}{1 - \frac{1}{4Q^2}}} \cdot cos\left(2\pi f_0 \cdot \sqrt{1 - \frac{1}{4Q^2}} \cdot t - \phi\right) \tag{29}$$

As in (29), the voltage response for an impulse current consists of the sinusoidal term with exponential decay and the impulse term multiplied by R_2. If the resistance is low, the first term is close to zero due to low R_2 and the square root term ~1 because of high Q. Then, the voltage droop is proportional to $1/C$ as in (1). However, if the resistance is appreciable, due to high R_2 and low Q, the first term and square root term are no longer zero and unity, respectively, resulting in the maximum voltage droop differing from 1/C proportionality shown in (1). Therefore, the resistance, especially R_2 can cause significant deviations in the droop calculations as compared to the estimations in (1).

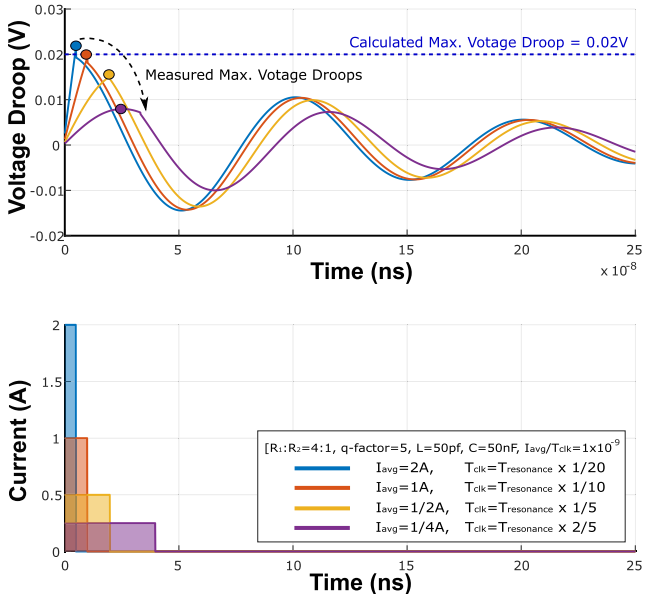

FIGURE 8. Change of the voltage droop depending on the different pulse time duration.

Another factor we need to consider for the validity of the equations is the parameter of the current source. In (1), only the charge I_{avg}/f_{clk} is considered. However, although current pulses may have the same charge, their time duration may differ. Then, for $0 < t \leq a$, the voltage response for a pulse current becomes the same as (17). In addition, when $t > a$, the voltage response becomes:

$$v(t)_{impulse} = Z_0 \cdot \frac{(R_2 - R_1)}{\sqrt{((R_2 - R_1)^2}} \cdot \sqrt{\frac{(1 - \frac{1}{Q^2}\frac{R_1 R_2}{(R_1+R_2)^2})^2}{(1 - \frac{1}{4Q^2})}} \cdot e^{-\left(\frac{2\pi f_0}{2Q}\right)\cdot t} \cdot \left\{ cos\left(2\pi f_0 \cdot \sqrt{1 - \frac{1}{4Q^2}} \cdot (t - \phi)\right) - e^{-\left(\frac{2\pi f_0}{2Q}\right)\cdot a} \cdot cos\left(2\pi f_0 \cdot \sqrt{1 - \frac{1}{4Q^2}} \cdot (t - a) - \phi\right) \right\} \tag{30}$$

Based on (30), the voltage response is an exponentially decaying sinusoid and its amplitude and phase depend on the pulse time duration a, resulting in the amplitude of the voltage droops differing from (29).

Fig. 8 shows the voltage droops caused by the current pulses having the same charge but different time duration. Due to the same charge, the calculated maximum voltage droop for all current pulses is 20mV. If the time duration of a current pulse is relatively short compared to the resonant period T_0, the maximum voltage droops are close to 20mV. However, as the time duration increases beyond $0.1 * T_{resonance}$, the difference between calculated and simulated values increase significantly.

C. RESONANT CURRENT

The voltage droop caused by a rectangular-shaped resonant current depends on the first harmonic component [9]. Using Fourier series, the resonant current can be represented as:

$$i(t)_{resonance} = I_{resonance}\frac{a}{T_0} + \sum_{n=1}^{\infty}\frac{2\cdot I_{resonance}}{n\pi}\cdot sin(\frac{a}{T_0}n\pi)\cdot cos(\frac{2n\pi}{T_0}t) \tag{31}$$

where a, n, T_0, and ω_0 are pulse duration, harmonic number, resonance period, and angular frequency of the current, respectively. Substituting $n = 1$, $a = T_0/2$ into (31), we obtain the first harmonic function of the resonant current as:

$$i(t)_{1st} = \frac{2\cdot I_{resonance}}{\pi}\cdot cos(\omega_0 t) \tag{32}$$

where $I_{resonance}$ is the magnitude of the resonant current. Since the impedance at f_0 is Z_{peak}, the voltage response becomes:

$$v^*(t) = Z_{peak}\cdot\frac{2}{\pi}\cdot I_{resonance}\cdot cos(\omega_0 t) \tag{33}$$

Here, the peak to peak voltage is $Z_{peak}\cdot 4/\pi\cdot I_{resonance}$. From (33), the maximum voltage droop is as shown in (3).

However, if Q is low because of the high resistance, Z_{peak} from (7) becomes inaccurate [9]. This is because, with the resistance included, f_0 and Z_{peak} from (4),(7) are not the actual resonant frequency and peak impedance, respectively. The resonant frequency of the PDN circuit can be derived as:

$$f_{resonance} = \frac{1}{2\pi\sqrt{LC}}\cdot\sqrt{\frac{L-R_1^2C}{L-R_2^2C}} \tag{34}$$

Here, the resonant frequency makes the imaginary part of the admittance equal zero, where the admittance is given by:

$$Y = \frac{1}{R_1+j\omega L} + \frac{1}{R_2+\frac{1}{j\omega C}} \tag{35}$$

Therefore, the impedance at f_0 needs to be re-calculated by using the equation:

$$Z(f_0) = \frac{(R_1+j\omega_0 L)(R_2+\frac{1}{j\omega_0 C})}{(R_1+j\omega_0 L)+(R_2+\frac{1}{j\omega_0 C})} \tag{36}$$

Substituting (4)−(7) into (36), the impedance $Z(f_0)$ becomes

$$\begin{aligned} Z(f_0) &= \frac{\frac{L}{C}+R_1R_2+j\sqrt{\frac{L}{C}}(-R_1+R_2)}{R_1+R_2} \\ &= Z_{peak}+\frac{R_1R_2}{R_1+R_2}+j\cdot Q(-R_1+R_2) \end{aligned} \tag{37}$$

In (37), considering non-zero values for the resistances R_1 and R_2, the impedance at f_0 is different from Z_{peak} shown in (7), thereby, affecting significantly the voltage droop.

Additionally, with low Q, the voltage droop from higher current harmonics, which is not considered in (3), yields different voltage droops as compared to the expected value. The voltage droop response from a resonant current source can be calculated using the equation:

$$\begin{aligned} v(t) &= Z_{DC}\cdot\frac{I_{resonance}}{2} + \sum_{\substack{n=1\\ n=odd}}^{\infty} Z_{nf_0}\cdot sin(\frac{2n\pi}{T_0}t) \\ &= Z_{DC}\cdot\frac{I_{resonance}}{2} + Z_{f_0}\cdot\frac{2\cdot I_{resonance}}{\pi}\cdot sin(\omega_0 t) \\ &\quad + Z_{3f_0}\cdot\frac{2\cdot I_{resonance}}{3\cdot\pi}\cdot sin(3\omega_0 t) \\ &\quad + Z_{5f_0}\cdot\frac{2\cdot I_{resonance}}{5\cdot\pi}\cdot sin(5\omega_0 t)+\cdots \end{aligned} \tag{38}$$

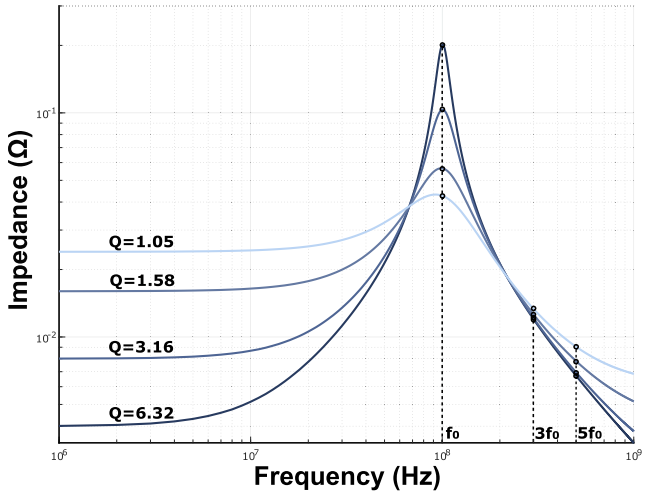

FIGURE 9. Impedance profiles of the PDN circuit depending on Q.

TABLE 3. Impedance values at each current harmonic depending on Q.

Frequency (Harmonic)	Impedance (Magnitude)			
	Q=6.32	Q=3.16	Q=1.58	Q=1.05
f_0 (1st)	201mΩ	103mΩ	56mΩ	43mΩ
$3f_0$ (3rd)	12mΩ	12mΩ	13mΩ	13mΩ
$5f_0$ (5th)	7mΩ	7mΩ	8mΩ	9mΩ

Here, the voltage droop depends on the impedance values at each frequency. As shown in Fig. 9 and Table 3, when Q is high, there are large differences between the impedance values of the first harmonic and higher harmonics. However, as Q decreases, the differences become smaller leading to an increase in the effect of voltage droops arising from higher harmonics.

D. ARBITRARY TRANSIENT CURRENT

The impulse, step and, periodic current sources can be used to represent an arbitrary current source. Hence, the voltage response for an arbitrary current can be obtained using a combination of (17), (30), and (38). This can provide a degree of freedom to set an arbitrary transient load current depending on IC operations, and the obtained voltage response from the customized transient current source can be used as a figure of merit for PDNs.

Fig. 10 provides an example of an arbitrary current source in ICs and the resulting voltage droop. Since the transient

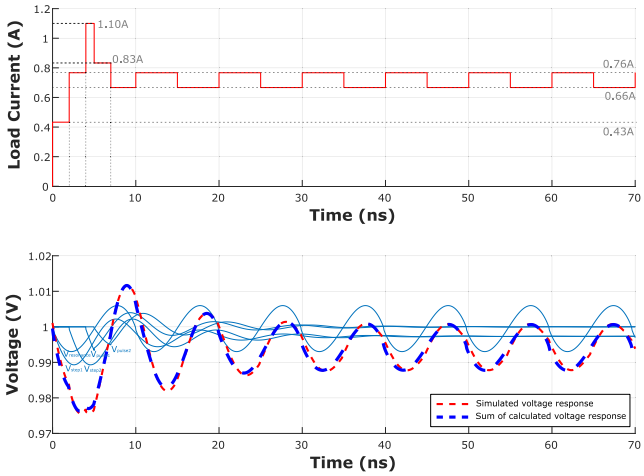

FIGURE 10. Voltage droop from an arbitrary current consisting of step, pulse, and resonant currents.

current can be represented as the sum of step, pulse, and resonance currents, the voltage response can be written as:

$$V_{droop}(t) = V_{step1}(t) + V_{step2}(t - T_{delay_1}) + V_{impulse1}(t - T_{delay_2}) + V_{impulse2}(t - T_{delay_3}) + V_{resonance}(t) \quad (39)$$

where T_{delay_1}, T_{delay_2}, and T_{delay_3} are the time instants when each current excitation occurs. The dotted line and solid line in Fig. 10 represent the analytical and simulated voltage response to the current excitation. The agreement in Fig. 10 indicates that the equations discussed earlier can be used to compute power supply accurately.

IV. ERROR ANALYSIS

Since (1)–(3) are simplified representations of the maximum voltage droop, they tend to be used widely. Our objective in this section is to quantify the error bounds based on the detailed equations derived in this work.

A. STEP CURRENT

As in (17), Q and resistance are parameters that can cause deviations from the voltage droop predicted using (2). Therefore, the error can be quantified by the dependence of Q and the ratio of PDN resistance to on-die resistance, regardless of other component parameters, as shown in Fig. 11a. The error is negligible with high Q, but increases significantly when it is around 2–3, meaning that the key parameter determining the error is Q.

Fig. 11b and 11c provide the specific range of Q and ratio of resistances that ensure low errors of 10% and 5%, respectively. If Q is greater than 2, the error in the predicted maximum voltage droop from (2) is less than 10%, regardless of the resistance ratio. In addition, with Q greater than 3, an error of less than 5% can be guaranteed if the resistance ratio is greater than 1.5:1. Even if Q is less than 2, the error can be less than 5%; however, the resistance ratio should be within a narrower range (1:2–1:4).

B. IMPULSE CURRENT

The error in the voltage droops computed from (1) arise from the resistance, pulse time duration T_{clk}, and Q, as shown in section III. Therefore, for constant values of these parameters, the error remains a fixed value. Among these parameters, R_2 and T_{clk} play a major role in causing a deviation from the actual value, as shown in Fig. 12a. Here, R_2 and T_{clk} are expressed in terms of ratios to the characteristic impedance Z_0 and resonant period $T_{resonance}$, respectively, for generalization.

The conditions to ensure errors of 10% and 5% are provided in Fig. 12b and 12c, respectively. The range of parameters varies depending on Q, but has little to no effect on determining the error. To ensure errors of less than 10% and 5%, the ratio of $T_{resonance}$ to T_{clk} needs to be at least 7:1 and 8:1, respectively, and the resistance ratio should be within the provided range for each time ratio.

C. RESONANT CURRENT

Fig. 13a shows the error dependence on Q and the resistance ratio, which can greatly affect the voltage droop, as in (37). As in the case of step current, the error is only close to zero when Q is high; however, the error increases significantly if Q decreases beyond a certain bound. Fig. 13b and 13c provide the range of Q and resistance ratio over which errors of 10% and 5% can be guaranteed. If Q is greater than 1.5, we can use (3) to predict the maximum voltage droop and expect an

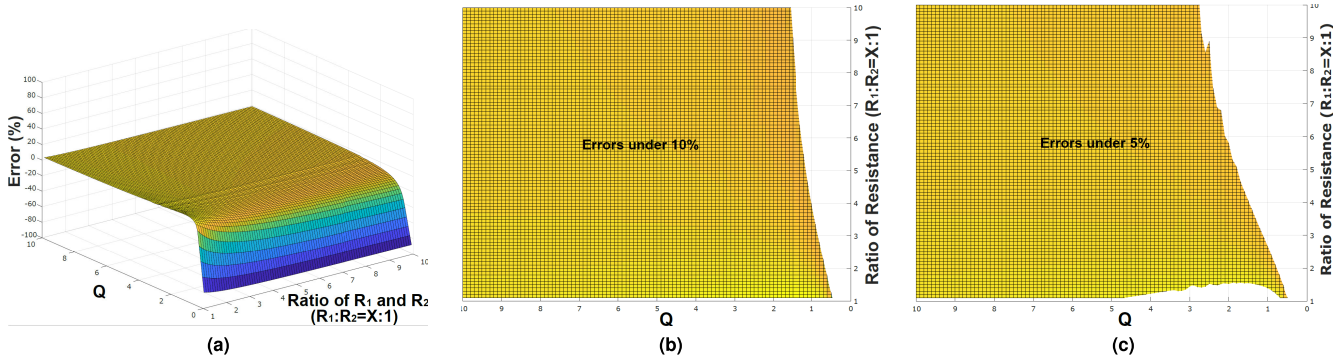

FIGURE 11. (a) Error in maximum voltage droop from a step current predicted by (2). (b) Parameters to achieve an error of less than 10%. (c) Parameters to achieve an error of less than 5%.

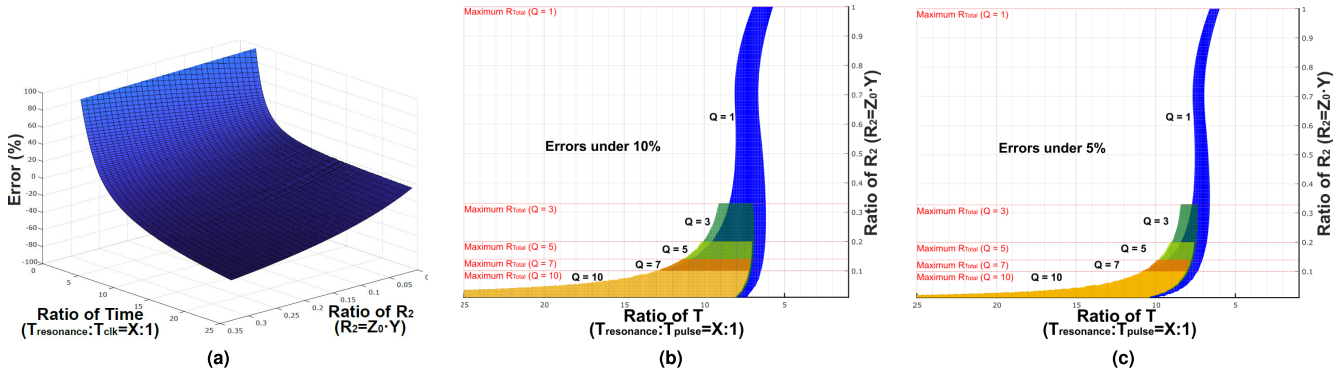

FIGURE 12. (a) Error in maximum voltage droop from an impulse current predicted by (1). (b) Parameters to achieve an error of less than 10%. (c) Parameters to achieve an error of less than 5%.

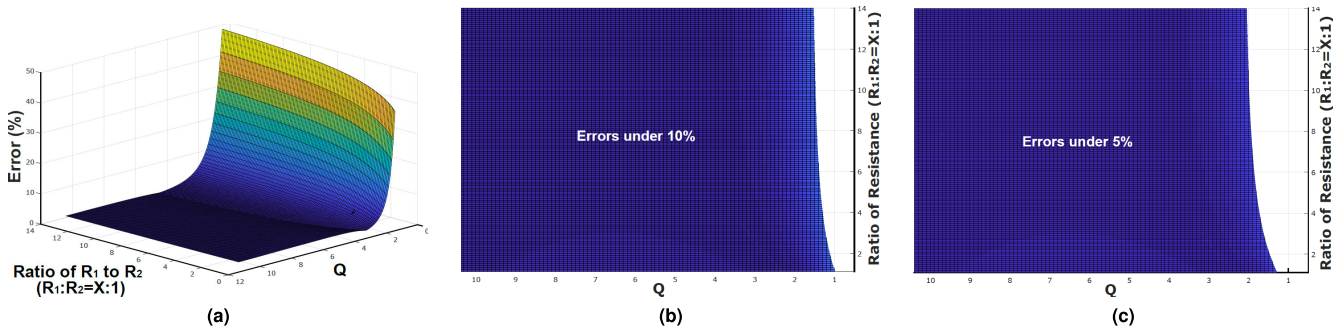

FIGURE 13. (a) Error in maximum voltage droop from a resonant current predicted by (3). (b) Parameters to achieve an error of less than 10%. (c) Parameters to achieve an error of less than 5%.

error of less than 10%. To obtain the predicted value with less than 5% error, Q needs to be greater than 2.

V. RISE TIME EFFECTS

In the previous sections, we consider an ideal step current. To be more realistic, we include the current rise time and evaluate its effect on the maximum voltage droop. Fig. 14 shows the voltage droops from step currents with various rise times in the PDN circuit. For a short rise time of 1 or 2 ns, the maximum voltage droop is similar to that of an ideal step current source. However, for rise time larger than 4 ns, the difference in maximum voltage droop caused by the ideal step becomes significant; for example, the maximum voltage droop becomes 18.1 mV for a rise time of 6 ns, which is almost half the value obtained from a step current source. This is an important effect, as currents with multiple rise times are possible in typical computer systems.

To demonstrate the effect of rise time, we analyze the change in the current envelope in the frequency domain as a function of rise time. A step current with a rise time can be regarded as a ramp current. Then, the envelope of the current harmonics in the frequency domain is [12]:

$$Envelope = 2\frac{I_0 T_w}{T}\left|\frac{sin(\pi T_w f)}{\pi T_w f}\right|\left|\frac{sin(\pi \tau f)}{\pi \tau f}\right| \tag{40}$$

where I_0, T, T_w, and τ are the current level, pulse period, pulse width, and rise time, respectively.

As shown in Fig. 15, there is an additional decrease in the envelope of the current harmonics due to the effect of

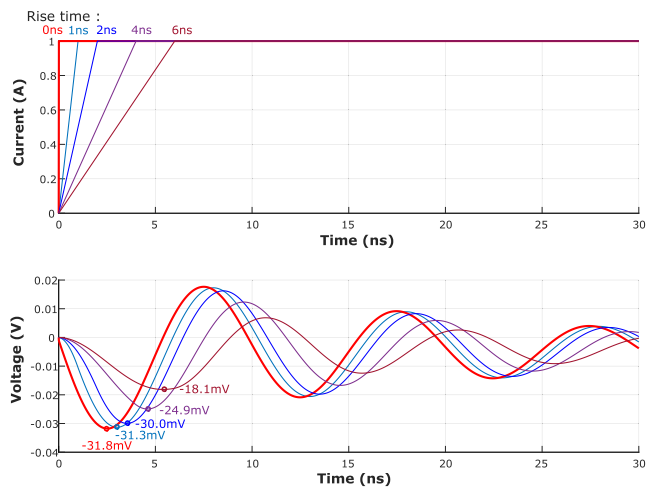

FIGURE 14. Change in voltage droop from step current depending on rise time.

current rise time τ when the frequency is higher than $1/\pi\tau$. Therefore, if the resonant frequency f_0 is higher than $1/\pi\tau$, the decreased magnitude of the envelope needs to be applied to (2), resulting in the following equation:

$$\begin{aligned} V_{step} &= \frac{1}{\pi \tau f_0} \cdot Z_0 \cdot I_{step} \\ &= \frac{1}{\pi \tau \cdot \frac{1}{2\pi\sqrt{LC}}} \cdot \sqrt{\frac{L}{C}} \cdot I_{step} \\ &= \frac{2L}{\tau} \cdot I_{step} \quad (when\, f_0 > 1/\pi\tau) \end{aligned} \tag{41}$$

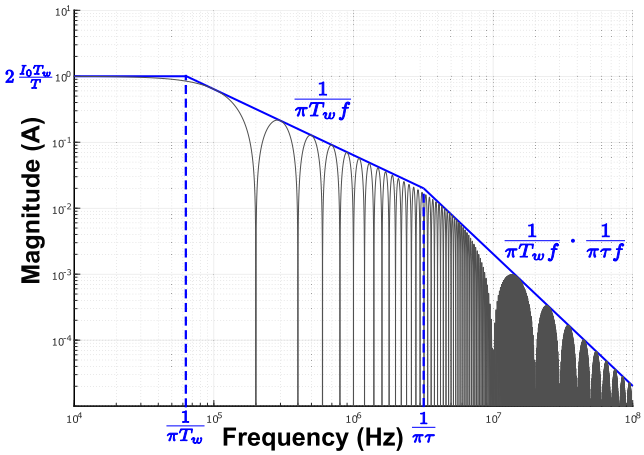

FIGURE 15. Envelope of step current with rise time in the frequency domain.

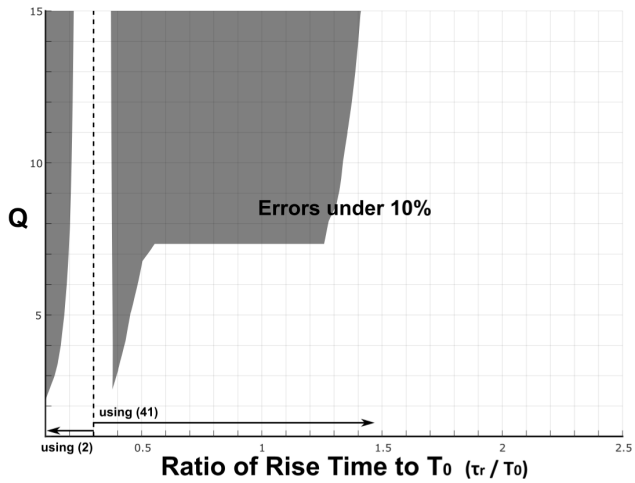

FIGURE 16. The condition of Q and current rise time for an error of less than 10% using (2) and (41).

where L, τ, and I_{step} are the PDN inductance, current rise time, and the level of current step.

Fig. 16 shows the parameter values of the PDN and current over which the error in predicted values is less than 10% when using (2) and (41). For a current rise time of less than $0.1 \cdot T_{resonance}$, equation (2) can still be used because there is a large difference between the resonant frequency of the PDN and $1/\pi\tau$. If the current rise time is greater than $0.4 \cdot T_{resonance}$ and less than $1.2 \cdot T_{resonance}$, proposed equation (41) can predict the maximum voltage droop with an error of less than 10% if Q is greater than 8.

VI. CONCLUSION

This article proposes a method to predict the maximum voltage droops caused by three fundamental current sources in ICs. The prediction equations are validated and their associated errors are analyzed based on the parameters of the PDN circuit and current sources. The voltage response from each current source can be computed with a minimal error by using the derived equations that include the parameters Q, resistance, and pulse time duration, which have not been considered previously. In addition, the effect of the current rise time is considered to accurately predict the maximum voltage droop from a step current. For the proper use of the simplified representations of the maximum voltage droop, the error bounds of the equations have been quantified by clarifying the factors leading to errors in each equation. The solutions presented in this article are based on rigorous derivations, and therefore provide reliable predictions of the maximum voltage droop.

REFERENCES

[1] C. Thibeault and G. Gagnon, "On the analysis and the mitigation of power supply noise and power distribution network impedance variation for scan-based delay testing techniques," *IEEE Trans. Very Large Scale Integr. (VLSI) Syst.*, vol. 26, no. 7, pp. 1377–1390, Jul. 2018.

[2] K. Chang, S. Das, S. Sinha, B. Cline, G. Yeric, and S. K. Lim, "System-level power delivery network analysis and optimization for monolithic 3-D ICs," *IEEE Trans. Very Large Scale Integr. (VLSI) Syst.*, vol. 27, no. 4, pp. 888–898, Apr. 2019.

[3] J. Chen, H. Kando, T. Kanamoto, C. Zhuo, and M. Hashimoto, "A multicore chip load model for PDN analysis considering voltage–Current-timing interdependency and operation mode transitions," *IEEE Trans. Compon., Packag., Manuf. Technol.*, vol. 9, no. 9, pp. 1669–1679, Sep. 2019.

[4] J. Jo, S. Kim, S. Lee, and S. Pae, "System-level practical dynamic voltage drop simulation with IC internal VRM," in *Proc. IEEE 20th Workshop Signal Power Integrity (SPI)*, May 2016, pp. 1–4.

[5] F. Ye, F. Firouzi, Y. Yang, K. Chakrabarty, and M. B. Tahoori, "On-chip voltage-droop prediction using support-vector machines," in *Proc. IEEE 32nd VLSI Test Symp. (VTS)*, Apr. 2014, pp. 1–6.

[6] J. Kim, L. Li, S. Wu, H. Wang, Y. Takita, H. Takeuchi, K. Araki, J. Fan, and J. L. Drewniak, "Closed-form expressions for the maximum transient noise voltage caused by an IC switching current on a power distribution network," *IEEE Trans. Electromagn. Compat.*, vol. 54, no. 5, pp. 1112–1124, Oct. 2012.

[7] B. Zhao, C. Huang, K. Shringarpure, J. Fan, B. Archambeault, B. Achkir, S. Connor, M. Cracraft, M. Cocchini, A. Ruehli, and J. Drewniak, "Analytical PDN voltage ripple calculation using simplified equivalent circuit model of PCB PDN," in *Proc. IEEE Symp. Electromagn. Compat. Signal Integrity*, Mar. 2015, pp. 133–138.

[8] J. Kim, Y. Takita, K. Araki, and J. Fan, "Improved target impedance for power distribution network design with power traces based on rigorous transient analysis in a handheld device," *IEEE Trans. Compon., Packag., Manuf. Technol.*, vol. 3, no. 9, pp. 1554–1563, Sep. 2013.

[9] L. D. Smith and E. Bogatin, *Principles of Power Integrity for PDN Design*. Upper Saddle River, NJ, USA: Prentice-Hall, 2017.

[10] M. Swaminathan and E. Engin, *Power Integrity Modeling and Design for Semiconductors and Systems*. London, U.K.: Pearson, 2007.

[11] L. D. Smith and Y. Cao, "A convolution technique for verifying acceptable PTPX current waveforms for PDN voltage droops," in *Proc. DesignCon*, 2018, pp. 1–21.

[12] N. Oswald, B. H. Stark, D. Holliday, C. Hargis, and B. Drury, "Analysis of shaped pulse transitions in power electronic switching waveforms for reduced EMI generation," *IEEE Trans. Ind. Appl.*, vol. 47, no. 5, pp. 2154–2165, Sep. 2011.

SEUNGHYUP HAN received the B.S. degree in electronic and electrical engineering from Sungkyunkwan University, Suwon, South Korea, in 2011. He is currently pursuing the Ph.D. degree with the Georgia Institute of Technology, Atlanta, GA, USA.

He has been a Staff Engineer with the Mobile Communication Device Department, Samsung Electronics Company Ltd., Suwon, where he is also involved in the power and signal integrity, power efficient system design, and power management systems. His current research interests include analysis of power supply noise and signal, power, and thermal integrity in designs of power delivery networks.

OSAMA WAQAR BHATTI received the bachelor's degree in electrical engineering from the National University of Sciences and Technology, Islamabad, Pakistan, in 2017. He is currently pursuing the Ph.D. degree with the Georgia Institute of Technology, Atlanta, GA, USA.

His current research interest includes designing machine learning algorithms for signal and power integrity applications.

MADHAVAN SWAMINATHAN (Fellow, IEEE) received the M.S. and Ph.D. degrees in electrical engineering from Syracuse University, in 1989 and 1991, respectively.

He is currently the John Pippin Chair of Microsystems Packaging and Electromagnetics with the School of Electrical and Computer Engineering (ECE), a Professor of ECE with a joint appointment at the School of Materials Science and Engineering (MSE), and the Director of the 3D Systems Packaging Research Center (PRC), Georgia Tech (GT). He is also the Site Director of the NSF Center for Advanced Electronics through Machine Learning (CAEML) and the Theme Leader of the Heterogeneous Integration, SRC JUMP ASCENT Center. He formerly held the position of Founding Director at the Center for Co-Design of Chip, Package, System (C3PS), the Joseph M. Pettit Professor of Electronics at ECE, and the Deputy Director of the Packaging Research Center (NSF ERC), GT. Prior to joining GT, he was with IBM working on packaging for supercomputers. He is the author of more than 500 refereed technical publications, holds 30 patents, a primary author and a co-editor of three books, a founder and a co-founder of two start-up companies.

Dr. Swaminathan's research has been recognized with 22 best paper and best student paper awards. In addition, his most recent awards include the D. Scott Wills ECE Distinguished Mentor Award, in 2018, the GT Outstanding Achievement in Research Program Development Award, in 2017, the Distinguished Alumnus Award from the National Institute of Technology Tiruchirappalli (NITT), India, in 2014, and the Outstanding Sustained Technical Contribution Award from the IEEE Components, Packaging, and Manufacturing Technology Society, in 2014. He is a Founder of the IEEE Conference Electrical Design of Advanced Packaging and Systems (EDAPS), a premier conference sponsored by the EPS society. He has served as the Distinguished Lecturer for the IEEE EMC Society.